Journal of Sound and Vibration (1999) **223**(3), 355–378
Article No. jsvi.1998.2126, available online at http://www.idealibrary.com on IDEAL®

NOISE PROPAGATION FROM A CUTTING OF ARBITRARY CROSS-SECTION AND IMPEDANCE

A. T. PEPLOW

*Department of Mathematical Sciences, University of the West of England, Coldharbour Lane, Frenchay, Bristol BS*16 1*QY, England*

AND

S. N. CHANDLER-WILDE

*Department of Mathematics and Statistics, Brunel University, Uxbridge, Middlesex, UB*8 3*PH, England*

(*Received* 18 *June* 1998, *and in final form* 24 *November* 1998)

A boundary integral equation is described for the prediction of acoustic propagation from a monofrequency coherent line source in a cutting with impedance boundary conditions onto surrounding flat impedance ground. The problem is stated as a boundary value problem for the Helmholtz equation and is subsequently reformulated as a system of boundary integral equations via Green's theorem. It is shown that the integral equation formulation has a unique solution at all wavenumbers. The numerical solution of the coupled boundary integral equations by a simple boundary element method is then described. The convergence of the numerical scheme is demonstrated experimentally. Predictions of A-weighted excess attenuation for a traffic noise spectrum are made illustrating the effects of varying the depth of the cutting and the absorbency of the surrounding ground surface.

1. INTRODUCTION

A boundary integral equation formulation for the two-dimensional Helmholtz equation in a locally-perturbed half plane is developed to calculate sound propagation out of a cutting of arbitrary cross-section and surface impedance onto surrounding flat rigid or homogeneous ground. Specifically, the case considered is that of propagation from a monofrequency coherent line source in a cutting which is assumed to be straight and infinitely long with cross-section and surface treatment that do not vary along its length. The impedance is allowed to vary in the cutting in the plane perpendicular to the line source so that it is possible to model, for example, a road running down the centre of the cutting, with grass banks on either side.

0022–460X/99/230355 + 24 $30.00/0

Let $U := \{(x_1, x_2): x_2 > 0\}$ denote the upper half plane and suppose that $\mathbf{x}^{(1)} = (a, 0)$, $\mathbf{x}^{(2)} = (b, 0) \in \partial U$ with $a < b$, $\gamma_2 := \{(x_1, 0) : a \leqslant x_1 \leqslant b\}$ and $\gamma_3 := \partial U \setminus \gamma_2$. Let γ_1 be any piecewise smooth arc connecting and including $x^{(1)}$ and $x^{(2)}$ which lies entirely (apart from its end-points $\mathbf{x}^{(1)}$ and $\mathbf{x}^{(2)}$) below the closed upper half plane $\bar{U}$. Then $\gamma_1 \cup \gamma_3$ divides the plane into two regions. Let D be the region above $\gamma_1 \cup \gamma_3 = \partial D$, containing U, and let S be the region enclosed by γ_1 and γ_2; see Figure 1.

The solution of the boundary value problem (BVP) consisting of the Helmholtz equation in the region D with an impedance or Robin boundary condition on ∂D and its reformulation as a boundary integral equation (BIE) will be discussed. It will be assumed throughout that γ_3 has a constant admittance β_c with $\beta_c = 0$ (rigid boundary) or $\mathrm{Re}\,\beta_c > 0$ (energy absorbing boundary).

Boundary integral equation formulations for this problem but assuming an entirely rigid boundary (leading to a Neumann boundary condition) are given in the context of predicting water-wave climates in harbours in reference [1]. The harbour resonance problem is of importance in coastal engineering, where small harbour oscillations excite large motions in ship-mooring causing considerable damage. To minimize such events the characteristics of harbour response must be determined. Hwang and Tuck [1] adopt a single-layer potential method which determines the wave-induced oscillations using a distribution of sources along the boundary of the harbour (γ_1) and coastline (γ_3) with unknown source strengths. Lee [2] applies Green's second theorem in both the regions inside and outside the harbour, S and U, respectively, which is the method adopted in this study, and matches the wave-amplitudes and their normal derivatives at the harbour entrance (γ_2). The same integral equation approach as Lee [2] is used by Shaw [3]. These methods were compared with experimental scale models for rectangular basins and real harbours and good agreement was found.

A related problem is the case when γ_1 lies entirely within rather than below the upper half-plane U, and this case has been used as a model of acoustic propagation over outdoor noise barriers (see e.g., reference [4]). In this case a formulation as a single integral equation over γ_1 is possible using the impedance

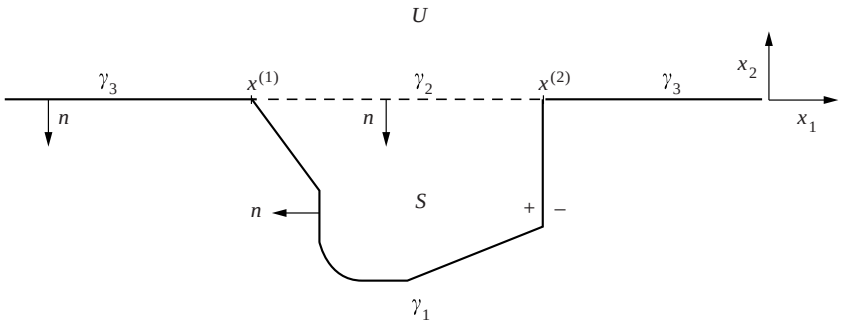

Figure 1. Geometry of model.

Green's function for the upper half-plane U as fundamental solution. This approach fails when γ_1 lies below the upper half-plane U since this Green's function is undefined at points outside U. For a recent general review of the application of boundary integral equation methods in modelling outdoor noise problems see reference [5].

Section 2 describes the formulation of the boundary value problem in the unbounded domain. The boundary integral equation is formulated in section 3, derived from the BVP via applications of Green's second theorem in U and S. This method coincides with that of Hwang and Tuck [1] when the boundary is completely rigid. For $\beta_c \neq 0$ the fundamental solution in the upper half plane U used is the Green's function G_{β_c} for the Helmholtz equation with impedance boundary condition of constant admittance β_c on the boundary ∂U. The integral equation formulation is a coupled system of three integral equations, two second-kind Fredholm equations and one first-kind Fredholm equation. Equivalence of this system with the original boundary value problem, and thus uniqueness of solution at all wavenumbers of the integral equation formulation is then established.

The numerical method of solution of the BIE implemented is a product integration method [6] using the product mid-point rule and is presented in section 4. The convergence of the numerical scheme is demonstrated experimentally in section 5. Predictions of attenuation, in excess of that in free-field propagation, are presented for a traffic noise spectrum, in section 6, for site configurations where the traffic noise is propagating out of a cutting and onto surrounding flat ground. To illustrate the scope of the mathematical model calculations are made which examinine the effect on the excess attenuation of the depth of the cutting and of the effective flow resistivity of the surrounding flat ground surface.

The discussion and numerical scheme is limited throughout to the case of a coherent line source of sound, which has the advantage that the mathematical problem is two-dimensional so that the computational problem is feasible. Of course a traffic noise stream is more realistically modelled as an incoherent line source, especially as regards calculation of L_{eq} values, and a single vehicle is more realistically modelled as a point source of sound. Both these cases, via partial Fourier transformation, can be reduced to the solution of a sequence of two-dimensional problems with a coherent line source of sound which can then be treated using the formulation and numerical scheme described: see Duhamel [7] or Chandler-Wilde [5] for details.

2. FORMULATION AS A BOUNDARY VALUE PROBLEM

Given a source at $\mathbf{x}_0$ somewhere in the region D, the pressure induced at $\mathbf{x}$, denoted by $p(\mathbf{x})$ (a harmonic time dependence e^{-iwt} is assumed and suppressed throughout), may be written as the sum of the incoming field and the scattered field, that is $p(\mathbf{x}) = G_f(\mathbf{x}, \mathbf{x}_0) + P(\mathbf{x})$ where $G_j(\mathbf{x}, \mathbf{x}_0) := -i/4H_0^{(1)}(k|\mathbf{x} - \mathbf{x}_0|)$ ($H_0^{(1)}$ is the Hankel function of the first-kind of order zero and k the wavenumber) is the

free-field Green's function. The pressure p is assumed to satisfy the following BVP:

BVP1. Given $k>0$ and an impedance over the ground, β, such that β is constant $(=\beta_c)$ on γ_3, the flat surface, find p such that

$$p(\mathbf{x}) = P(\mathbf{x}) + G_f(\mathbf{x}, \mathbf{x}_0), \qquad \mathbf{x} \in \bar{D}\backslash\{\mathbf{x}_0\}, \tag{1}$$

and such that p satisfies the Helmholtz equation,

$$(\nabla^2 + k^2)p(\mathbf{x}) = 0, \qquad \mathbf{x} \in D\backslash\{\mathbf{x}_0\}, \tag{2}$$

the impedance boundary condition,

$$\frac{\partial p(\mathbf{x})}{\nabla n} = \mathrm{i}k\beta(\mathbf{x})p(\mathbf{x}), \qquad \mathbf{x} \in \partial D, \tag{3}$$

and the Sommerfeld radiation conditions

$$\partial p(\mathbf{x})/\partial r - \mathrm{i}kp(\mathbf{x}) = o(r^{-1/2}),$$
$$p(\mathbf{x}) = O(r^{-1/2}), \tag{4}$$

uniformly in $\mathbf{x}$ as $r := |x| \to \infty$.

The above boundary value problem has at most one solution—see references [8, 9] where the existence of a solution is also established under the assumption that at corners of ∂D the interior and exterior angles do not vanish.

3. REFORMULATION OF THE BOUNDARY VALUE PROBLEM AS AN INTEGRAL EQUATION

Let γ be a simple open or closed curve. Given a function ϕ defined on γ, the function u defined by

$$u(\mathbf{x}) = S_\gamma\phi(\mathbf{x}) = \int_\nu G_f(\mathbf{x}, \mathbf{y})\phi(\mathbf{y})\mathrm{d}s(\mathbf{y}), \qquad \mathbf{x} \in \mathrm{R}^2, \tag{5}$$

is called the acoustic single-layer potential and the function v defined by

$$v(x) = K_\gamma\phi(\mathbf{x}) = \int_\nu \frac{\partial G_f\mathbf{x}, \mathbf{y})}{\partial n(\mathbf{y})}\phi(\mathbf{y})\mathrm{d}s(\mathbf{y}), \qquad \mathbf{x} \in \mathrm{R}^2, \tag{6}$$

is called the acoustic double-layer potential.

Denote by $G_{\beta_c}(\mathbf{x}, \mathbf{x}_0)$ the fundamental solution to the Helmholtz equation in $\bar{U}$ which satisfies the Sommerfeld radiation conditions (4) and the impedance boundary condition $\partial G_{\beta_c}(\mathbf{x}, \mathbf{x}_0)/\partial n(\mathbf{x}) = \mathrm{i}k\beta_c G_{\beta_c}(\mathbf{x}, \mathbf{x}_0)$ on $\mathbf{x} \in \partial U$.

Analytical expressions for $G_{\beta_c}(\mathbf{x}, \mathbf{x}_0)$ have been obtained by Rasmussen [10], Filippi [11] (and see Habault [12]), and by Chandler-Wilde and Hothersall [13]. From reference [13] one has that, for $\mathbf{x}, \mathbf{x}_0 \in \bar{U}$, $\mathbf{x} \neq \mathbf{x}_0$,

$$G_{\beta_c}(\mathbf{x}, \mathbf{x}_0) = G_f(\mathbf{x}, \mathbf{x}_0) + G_f(\mathbf{x}, \mathbf{x}_0') + P_{\beta_c}(k(\mathbf{x} - \mathbf{x}_0')),$$

where $\mathbf{x}_0'$ is the image of $\mathbf{x}_0$ in the x_1-axis and, for $-\infty < \xi < +\infty$, $\eta \geqslant 0$, $\beta_c \neq 1$, $P_{\beta_c}((\xi, \eta))$ is given by

$$P_{\beta_c}((\xi, \eta)) = \frac{\beta_c e^{i\rho}}{\pi} \int_0^\infty t^{-1/2}\, e^{-\rho t} g(t)\, dt + \frac{\beta_c\, e^{i\rho(1-a_+)}}{2\sqrt{1-\beta_c^2}} \operatorname{erfc}(e^{-i\pi/4}\sqrt{\rho a_+}), \qquad (7)$$

with $\rho = (\xi^2 + \eta^2)^{1/2}$, $\gamma = \eta/\rho$, $a_+ = 1 + \beta_c\gamma - \sqrt{1-\beta_c^2}\sqrt{1-\gamma^2}$, erfc the complementary error function, and

$$g(t) = \frac{-\beta_c - \gamma(1 + it)}{\sqrt{t - 2i}(t^2 - 2i(1 + \beta_c\gamma)t - (\beta_c + \gamma)^2)} - \frac{e^{-i\pi/4}\sqrt{a_+}}{2\sqrt{1-\beta_c^2}(t - ia_+)}.$$

(Note that all the complex square roots in the above expressions are to be taken with non-negative real part.) The above formulae for $G_{\beta_c}(\mathbf{x}, \mathbf{x}_0)$ are used for all the numerical calculations reported later in this paper. The integral in (7) can be evaluated efficiently and accurately by Gauss–Laguerre quadrature as described and analysed in reference [13].

Given ϕ defined on γ_2, call the function

$$w(\mathbf{x}) = S^{\beta_c}\phi(\mathbf{x}) = \int_{\nu_2} G_{\beta_c}(\mathbf{x}, \mathbf{y})\phi(\mathbf{y})\, ds(\mathbf{y}), \qquad \mathbf{x} \in \bar{U} \qquad (8)$$

the modified acoustic single-layer potential.

Henceforth, abbreviate S_{γ_i} as S_i and K_{γ_i} as K_i, for $i = 1, 2$ and in the following define single and double-layer potential operators over open arcs. For $i = 1, 2$ let $L_2(\gamma_i)$ denote the set of functions square integrable on γ_i. Define single-layer potential operators from $L_2(\gamma_i)$ to $L_2(\gamma_j)$, for $i, j = 1, 2$, by

$$S_{ij}(\mathbf{x}) = \int_{\gamma i} G_f(\mathbf{x}, \mathbf{y})\phi(\mathbf{y})\, ds(\mathbf{y}), \qquad \mathbf{x} \in \gamma_j, \qquad (9)$$

and define double-layer potential operators from $L_2(\gamma_i)$ to $L_2(\gamma_j)$, for $i, j = 1, 2$, by

$$K_{ij}\psi(\mathbf{x}) = \int_{\gamma i} \frac{\partial G_f(\mathbf{x}, \mathbf{y})}{\partial n(\mathbf{y})} \psi(\mathbf{y})\, ds(\mathbf{y}), \qquad \mathbf{x} \in \gamma_j. \qquad (10)$$

Define a modified single-layer potential operator by

$$S_{22}^{\beta_c}\phi(\mathbf{x}) = \int_{\gamma 2} G_{\beta_c}(\mathbf{x}, \mathbf{y})\phi(\mathbf{y})\, ds(\mathbf{y}), \qquad \mathbf{x} \in \gamma_2. \qquad (11)$$

For simplicity assume henceforth that $\mathbf{x}_0 \notin \nu_2$, so that $\mathbf{x}_0 \in D \setminus \gamma_2$. The integral formulation is first stated followed by its derivation.

Suppose that p satisfies BVP1. Then it can be shown that

$$p(\mathbf{x}) = \int_{\gamma 2} G_{\beta_c}(\mathbf{x}, \mathbf{y}) \left(\mathrm{i}k\beta_c p(\mathbf{y}) - \frac{\partial p(\mathbf{y})}{\partial n} \right) \mathrm{d}s(\mathbf{y}) + \eta(\mathbf{x}_0) G_{\beta_c}(\mathbf{x}, \mathbf{x}_0), \qquad \mathbf{x} \in \bar{U} \backslash \{\mathbf{x}_0\}, \tag{12}$$

where

$$\eta(\mathbf{x}_0) = \begin{cases} 1, & \mathbf{x}_0 \in U, \\ 0, & \mathbf{x}_0 \in S, \end{cases}$$

and

$$\begin{aligned} \varepsilon(\mathbf{x}) p(\mathbf{x}) = & \int_{\gamma_2} \left(G_f(\mathbf{x}, \mathbf{y}) \frac{\partial p(\mathbf{y})}{\partial n} - \frac{\partial G_f(\mathbf{x}, \mathbf{y})}{\partial n(\mathbf{y})} p(\mathbf{y}) \right) \mathrm{d}s(\mathbf{y}) \\ & + \int_{\gamma_1} p(\mathbf{y}) \left(\frac{\partial G_f(\mathbf{x}, \mathbf{y})}{\partial n(\mathbf{y})} - \mathrm{i}k\beta(\mathbf{y}) G_f(\mathbf{x}, \mathbf{y}) \right) \mathrm{d}s(\mathbf{y}) \\ & + (1 - \eta(\mathbf{x}_0)) G_f(\mathbf{x}, \mathbf{x}_0), \qquad x \in \bar{S} \backslash \{\mathbf{x}_0\}, \end{aligned} \tag{13}$$

where $\varepsilon(\mathbf{x}) = 1$, $\mathbf{x} \in S$, $= 0$, $\mathbf{x} \in \mathrm{R}^2 \backslash \bar{S}$, and $\varepsilon(\mathbf{x}) = 1/2$ at points $\mathbf{x} \in \partial S \backslash \{\mathbf{x}^{(1)}, \mathbf{x}^{(2)}\}$ which are not corner points.

To derive equation (12) Green's second theorem is applied to the functions $u = p$ and $v = G_{\beta_c}(\mathbf{x},.)$ in a region E consisting of that part of U contained in a large circle of radius R centred on the origin, $\mathbf{x}_0$. Since $\nabla^2 u + k^2 u = \delta_x$, $\nabla^2 v + k^2 v = \delta_{x_0}$ in a distributional sense in E, where $\delta_y(\mathbf{x}) = \delta(\mathbf{x} - \mathbf{y})$ and δ denotes the two-dimensional Dirac delta function, one obtains

$$u(\mathbf{x}) = \eta(\mathbf{x}_0) v(\mathbf{x}_0) + \int_{\partial E} \left(u \frac{\partial v}{\partial n} - v \frac{\partial u}{\partial n} \right) \mathrm{d}s, \tag{14}$$

where $\eta(\mathbf{x}_0) = 1$ for $\mathbf{x}_0 \in U = 0$, for $\mathbf{x}_0 \in S$. Thus, letting $R \to \infty$ in equation (14) one obtains for $\mathbf{x} \in U \backslash \{\mathbf{x}_0\}$,

$$p(\mathbf{x}) = \eta(\mathbf{x}_0) G_{\beta_c}(\mathbf{x}, \mathbf{x}_0) + \int_{\partial U} \left(p(\mathbf{y}) \frac{\partial G_{\beta_c}(\mathbf{x}, \mathbf{y})}{\partial n(\mathbf{y})} - G_{\beta_c}(\mathbf{x}, \mathbf{y}) \frac{\partial p(\mathbf{y})}{\partial n} \right) \mathrm{d}s(\mathbf{y}). \tag{15}$$

The part of the integral on the circular arc of radius R in equation (14) vanishes as $R \to \infty$ since u and v both satisfy the Sommerfeld radiation conditions (4).

Utilizing the boundary condition satisfied by p on δU (equation (3)) and by G_{β_c} on δU one obtains equation (12) for $\mathbf{x} \in U \backslash \{\mathbf{x}_0\}$. Using the continuity of p and that of the modified single layer potential the validity of (12) is extended from $U \backslash \{\mathbf{x}_0\}$ to $\bar{U} \backslash \{\mathbf{x}_0\}$.

To derive equation (13) apply Green's representation theorem [14] to p in S. Utilizing the boundary condition (3) satisfied by p on γ_1 one obtains equation (13) for $\mathbf{x} \in S \backslash \{\mathbf{x}_0\}$. Using the continuity of p in $\bar{D} \backslash \{\mathbf{x}_0\}$ and $\partial p / \partial n$ across γ_2 and standard jump relations for layer potentials [14] the validity of equation (13) is extended from $S \backslash \{\mathbf{x}_0\}$ to $\bar{S} \backslash \{\mathbf{x}_0\}$.

Equations (12) and (13) express the pressure in D in terms of the unknowns p and $\delta p/\partial n$ on γ_2 and p on γ_1. Let $p_1 := p|_{\gamma_1}$, $p_2 := p|_{\gamma_2}$ and $q := \mathrm{i}k\beta_c p_2 - \partial p/\partial n|_{\gamma_2}$. In terms of the integral operators defined above, and noting that $K_{22}p_2 = 0$, it has been shown that p_1, p_2 and q satisfy the following integral equation problem:

IEP1. Find $p_1 \in L_2(\gamma_1)$, $p_2 \in L_2(\gamma_2)$ and $q \in L_2(\gamma_2)$ such that

$$p_2 = S_{22}^{\beta_c} g_{\beta_c}, \tag{16}$$

$$\tfrac{1}{2}p_2 = K_{12}p_1 - \mathrm{i}kS_{12}(\beta p_1) + \mathrm{i}k\beta_c S_{22}p_2 - S_{22}q + g_2, \tag{17}$$

$$\tfrac{1}{2}p_1 = K_{11}p_1 - \mathrm{i}kS_{11}(\beta p_1) + \mathrm{i}k\beta_c S_{21}p_2 - S_{21}q - K_{21}p_2 + g_1, \tag{18}$$

where g_{β_c}, $g_2 \in C(\gamma_2)$, $g_1 \in C(\gamma_1)$ are defined by $g_{\beta_c}(\mathbf{x}) := \eta(\mathbf{x}_0)G_{\beta_c}(\mathbf{x}, \mathbf{x}_0)$, $g_2(\mathbf{x}) := (1-\eta(\mathbf{x}_0))G_f(\mathbf{x}, \mathbf{x}_0)$, $\mathbf{x} \in \gamma_2$, and $g_1(\mathbf{x}) := (1-\eta(\mathbf{x}_0))G_f(\mathbf{x}, \mathbf{x}_0)$, $\mathbf{x} \in \gamma_1$.

The above arguments show that the system of integral equations IEP1 has a solution, namely $p_1 := p|_{\gamma_1}$, $p_2 := p|_{\gamma_2}$ and $q := \mathrm{i}k\beta_c p_2 - (\partial p/\partial n)|_{\gamma_2}$, where p is the solution of the boundary value problem BVP1. But it is not immediately obvious that this is the only solution of IEP1: indeed, it is well known that integral equation formulations in acoustic scattering can suffer from non-uniqueness of solution at an infinite set of positive wavenumbers [14], which leads to inaccuracy and instability when the equations are solved numerically. It is shown below that this non-uniqueness of solution does not arise for the present formulation by arguing that, conversely, if p_1, p_2 and q satisfy IEP1 and p is defined by equations (12) and (13) then p satisfies BVP1. As a corollary of this result and that BVP1 is uniquely solvable one has immediately that IEP1 has exactly one solution for all wavenumbers $k > 0$. To simplify the argument somewhat we assume that ∂S has no corner points except at $\mathbf{x}^{(1)}$ and $\mathbf{x}^{(2)}$.

Thus, suppose that p_1, p_2 and q satisfy IEP1 and define $p: \bar{D}\backslash\{\mathbf{x}_0\} \to C$ by

$$p(\mathbf{x}) = S^{\beta_c}q(\mathbf{x}) + \eta(\mathbf{x}_0)G_{\beta_c}(\mathbf{x}, \mathbf{x}_0), \qquad \mathbf{x} \in \bar{U}, \tag{19}$$

$$\begin{aligned}\varepsilon(\mathbf{x})p(\mathbf{x}) = {} & K_1p_1(\mathbf{x}) - \mathrm{i}kS_1(\beta p_1)(\mathbf{x}) + \mathrm{i}k\beta_c S_2p_2(\mathbf{x}) - S_2q(\mathbf{x}) \\ & - K_2p_2(\mathbf{x}) + (1-\eta(\mathbf{x}_0))G_f(\mathbf{x}, \mathbf{x}_0), \qquad \mathbf{x} \in \bar{S}\backslash\gamma_2.\end{aligned} \tag{20}$$

It will be shown that p satisfies BVP1, and that $p_1 = p|_{\gamma_1}$, $p_2 = p|_{\gamma_2}$ and $q = \mathrm{i}k\beta_c p_2 - \partial p/\partial n|_{\gamma_2}$.

First of all, with p defined by equations (19) and (20), define P by equation (1), i.e., $P(\mathbf{x}) = p(\mathbf{x}) - G_f(\mathbf{x}, \mathbf{x}_0)$, $\mathbf{x} \in \bar{D}\backslash\{\mathbf{x}_0\}$. It is easy to see that P satisfies the Sommerfeld radiation and boundedness conditions (4) and the Helmholtz equation in U and in S, and it follows immediately from standard jump relations for layer potentials [14] and from the integral equations (16)–(18) that $p_2 = p|_{\gamma_2}$, $p_1 = p|_{\gamma_1}$, $q = \mathrm{i}k\beta_c p_2 - \partial p/\partial n|_{\gamma_2}$ and $\partial p/\partial n = \mathrm{i}k\beta_c p$ on γ_3 (for details see reference [9]).

To recover the boundary conditions on γ_1 satisfied by p and the Helmholtz equation in D it is shown first that the right-hand side of equation (20) is identically zero outside $\bar{S}$. Let

$$\Phi(\mathbf{x}) := K_1p_1(\mathbf{x}) - \mathrm{i}kS_1(\beta p_1)(\mathbf{x}) + \mathrm{i}k\beta_c S_2 p_2(\mathbf{x}) - S_2\, q(\mathbf{x}) \tag{21}$$

$$-K_2 p_2(\mathbf{x}) + (1 - \eta(\mathbf{x}_0))G_f(\mathbf{x}, \mathbf{x}_0), \qquad \mathbf{x} \in \mathrm{R}^2 \setminus \bar{S}. \tag{22}$$

Then Φ satisfies the Helmholtz equation and Sommerfeld radiation conditions and, from standard jump relations for layer potentials [14] and the integral equations (17) and (18), $\Phi(\mathbf{x}) \to 0$ as $\mathbf{x}$ approaches ∂S. Thus, Φ satisfies a radiation problem in the exterior of S with homogeneous Dirichlet data $\Phi = 0$ on ∂S and hence vanishes identically [15]. The boundary conditions on γ_1, are now recovered for standard jump relations applied to the right-hand side of equations (20) gives, on γ_1,

$$\frac{\partial p}{\partial n} = \mathrm{i}k\beta p + \frac{\partial \Phi}{\partial n} = \mathrm{i}k\beta p. \tag{23}$$

To see finally that p and its derivatives are continuous across γ_2 and that p satisfies the Helmholtz equations in the whole of D, let U_R, D_R denote the parts of U and D respectively contained in a large circle of radius R centred on the origin, with R large enough so that $\mathbf{x}_0 \in D_R$, $\gamma_2 \subset D_R$. Applying Green's representation theorem [14] in U_R one obtains that

$$\begin{aligned} \varepsilon_1(\mathbf{x})p(\mathbf{x}) = \int_{\partial U_R} \left(\frac{\partial \gamma_f(\mathbf{x}, \mathbf{y})}{\partial n(\mathbf{y})} p(\mathbf{y}) - G_f(\mathbf{x}, \mathbf{y}) \frac{\partial p(\mathbf{y})}{\partial n} \right) \mathrm{d}s(\mathbf{y}) \\ + \eta(\mathbf{x}_0)G_f(\mathbf{x}, \mathbf{x}_0), \qquad \mathbf{x} \in \mathrm{R}^2 \backslash \{\mathbf{x}_0\}, \end{aligned} \tag{24}$$

where

$$\varepsilon_1(\mathbf{x}) := \begin{cases} 1, & \mathbf{x} \in U_R, \\ 1/2, & \mathbf{x} \in \gamma_2, \\ 0, & \mathbf{x} \in (\mathrm{R}^2 \backslash \bar{U}_R). \end{cases} \tag{25}$$

Now add the right-hand side of equation (24) to the right-hand side of equation (20), noting that the right-hand side of equation (20) has the value $p(\mathbf{x})$ in S, the value $\frac{1}{2}p_2(\mathbf{x}) = \frac{1}{2}p(\mathbf{x})$ on γ_2, by equation (17), and the value $\Phi(\mathbf{x}) = 0$ in U, to find that

$$p(\mathbf{x}) = G_f(\mathbf{x}, \mathbf{x}) + \int_{\partial D_R} \left(\frac{\partial G_f(\mathbf{x}, \mathbf{y})}{\partial n(\mathbf{y})} p(\mathbf{y}) - G_f(\mathbf{x}, \mathbf{y}) \frac{\partial p(\mathbf{y})}{\partial n} \right) \mathrm{d}s(\mathbf{y}), \qquad x \in D_R. \tag{26}$$

It follows from this last equation that P and its derivatives are continuous across γ_2 and that P satisfies the Helmholtz equation in D_R and hence in D.

4. NUMERICAL SOLUTION OF THE INTEGRAL EQUATIONS

To solve the above system of integral equations (16)–(18) numerically first divide γ_1 and γ_2 into boundary elements. Approximate γ_1 by an open polygon consisting of N_1 straight-line elements $\gamma_1^1, \ldots, \gamma_1^{N_1}$ so that the end-points of the elements lie on the arc γ_1; see Figure 2. For $n = 1, 2, \ldots, N_1$, x_1^n denotes the mid-

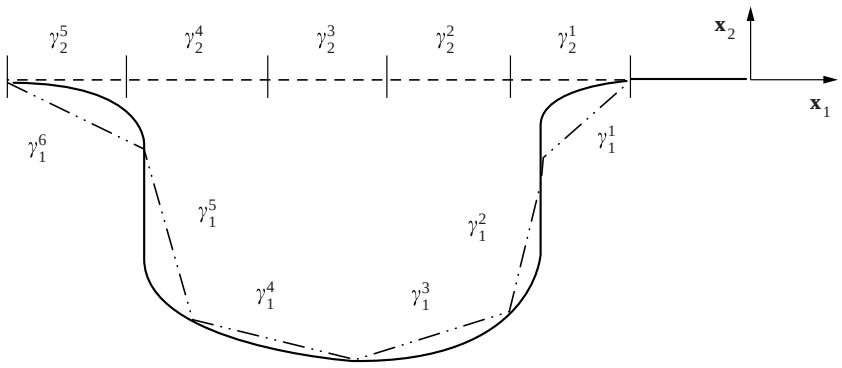

Figure 2. Cutting discretization

point and h_1^n the length of ν_1^n and $h_1 := \max h_1^n$. Similarly the straight line boundary γ_2 is divided into N_2 elements $\gamma_2^1, \ldots, \gamma_2^{N_2}$ and $\mathbf{x}_2^h$, h_2^n denote the mid-point and length of γ_2^n, and $h_2 := \max h_2^n$. Also, define $h := \max(h_1, h_2)$ and $N = (N_1, N_2)$.

Assuming that h, the maximum element length, is small enough so that p_1, β, and p_2, q are approximately constant on each element of γ_1 and γ_2, respectively, then the following approximations to equations (12) and (13) are valid:

$$p(\mathbf{x}) \approx \sum_{n=1}^{N_2} \int_{\gamma_2^n} G_{\beta_c}(\mathbf{x}, \mathbf{y})\ \mathrm{d}s(\mathbf{y}) q(\mathbf{x}_2^n) + \eta(\mathbf{x}_0) G_{\beta_c}(\mathbf{x}, \mathbf{x}_0), \qquad \mathbf{x} \in \bar{U} \backslash \{\mathbf{x}_0\}, \tag{27}$$

$$\begin{aligned} \varepsilon(\mathbf{x}) p(\mathbf{x}) \approx\ & \mathrm{i}k\beta_c \sum_{n=1}^{N_2} \int_{\gamma_2^n} G_f(\mathbf{x}, \mathbf{y})\ \mathrm{d}s(\mathbf{y}) p_2(\mathbf{x}_2^n) - \sum_{n=1}^{N_2} \int_{\gamma_2^n} G_f(\mathbf{x}, \mathbf{y})\ \mathrm{d}s(\mathbf{y}) q(\mathbf{x}_2^n) \\ & - \sum_{n=1}^{N_2} \int_{\gamma_2^n} \frac{\partial G_f(\mathbf{x}, \mathbf{y})}{\partial n(\mathbf{y})}\ \mathrm{d}s(\mathbf{y}) p_2(\mathbf{x}_2^n) + \sum_{n=1}^{N_1} \int_{\gamma_1^n} \frac{\partial G_f(\mathbf{x}, \mathbf{y})}{\partial n(\mathbf{y})}\ \mathrm{d}s(\mathbf{y}) p_1(\mathbf{x}_1^n) \\ & - \mathrm{i}k \sum_{n=1}^{N_1} \int_{\gamma_1^n} G_f(\mathbf{x}, \mathbf{y})\ \mathrm{d}s(\mathbf{y}) \beta(\mathbf{x}_1^n) p_1(\mathbf{x}_1^n) \\ & + (1 - \eta(x_0)) G_f(\mathbf{x}, \mathbf{x}_0), \qquad \mathbf{x} \in \bar{S} \backslash \{\mathbf{x}_0\}. \end{aligned} \tag{28}$$

The integrals in equations (27) and (28) are further replaced by approximations, for $i = 1, 2$,

$$a(\mathbf{x}, \gamma_i^n) \approx \int_{\gamma_i^n} G_f(\mathbf{x}, \mathbf{y})\, \mathrm{d}s(\mathbf{y}), \tag{29}$$

$$b(\mathbf{x}, \gamma_i^n) \approx \int_{\gamma_i^n} \frac{\partial G_f(\mathbf{x}, \mathbf{y})}{\partial n(\mathbf{y})} \mathrm{d}s(\mathbf{y}), \tag{30}$$

$$c(\mathbf{x}, \gamma_2^n) \approx \int_{\gamma_2^n} G_{\beta_c}(\mathbf{x}, \mathbf{y})\, \mathrm{d}s(\mathbf{y}), \tag{31}$$

to be defined shortly. Thus, p is approximated by p^N where p^N satisfies the approximate integral equations

$$p^N(\mathbf{x}) = \sum_{n=1}^{N_2} c(\mathbf{x}, \gamma_2^n) q^N(\mathbf{x}_2^n) + \eta(\mathbf{x}_0) G_{\beta_c}(\mathbf{x}, \mathbf{x}_0), \qquad \mathbf{x} \in \bar{U} \backslash \{\mathbf{x}_0\}, \tag{32}$$

$$\begin{aligned} \varepsilon(\mathbf{x}) p^N(\mathbf{x}) = & \sum_{n=1}^{N_2} [\{\mathrm{i}k\beta_c a(\mathbf{x}, \gamma_2^n) - b(\mathbf{x}, \gamma_2^n)\} p_2^N(\mathbf{x}_2^n) - a(\mathbf{x}, \gamma_2^n) q^N(\mathbf{x}_2^{\mathbf{n}})] \\ & + \sum_{n=1}^{N_1} \{b(\mathbf{x}, \gamma_1^n) - \mathrm{i}k\beta^N(\mathbf{x}_1^n) a(\mathbf{x}, \gamma_1^n)\} p_1^N(\mathbf{x}_1^n) \\ & + (1 - \eta(\mathbf{x}_0)) G_f(\mathbf{x}, \mathbf{x}_0), \qquad \mathbf{x} \in \bar{S} \backslash \{\mathbf{x}_0\}. \end{aligned} \tag{33}$$

In these equations q^N denotes a piecewise constant (constant on each ele-ment) approximation to q and $p_i^N := p^N|_{\gamma_i}$, $i = 1, 2$. The approximations to the layer-potentials $a(\mathbf{x}, \gamma_i^n)$, $b(\mathbf{x}, \gamma_i^n)$, $i = 1, 2$ and $c(\mathbf{x}, \gamma_i^n)$, are defined by simple product mid-point rules. Noting that $-\mathrm{i}/4\mathrm{H}_0^{(1)}(\mathbf{x}) = \ln|\mathbf{x}| A(\mathbf{x}) + B(\mathbf{x}) = \ln|\mathbf{x}| A(0) + C(\mathbf{x})$ where $A(z) = \mathrm{J}_0(\mathbf{z})/(2\pi)$ and $B(z)$ are even, entire functions (16), define, for $i = 1, 2$,

$$a(\mathbf{x}, \gamma_i^n) := \int_{\gamma_2^n} \ln(k|\mathbf{x} - \mathbf{y}|)\ \mathrm{d}s(\mathbf{y}) A(k|\mathbf{x} - \mathbf{x}_i^n|) + h_i^n B(k|\mathbf{x} - \mathbf{x}_i^n|), \qquad x \in \mathrm{R}^2, \tag{34}$$

$$b(\mathbf{x}, \gamma_i^n) := \frac{1}{2\pi} \int_{\gamma_i^n} \frac{(\mathbf{y} - \mathbf{x}) \cdot n(\mathbf{y})}{|\mathbf{y} - \mathbf{x}|^2}\ \mathrm{d}s(\mathbf{y}) + h_i^n C(k|\mathbf{x} - \mathbf{x}_i^n|), \qquad \mathbf{x} \in \mathrm{R}^2. \tag{35}$$

The integral in equation (35) can be evaluated exactly; its magnitude, in fact, is the angle at $\mathbf{x}$ subtended by the arc y_i^n, provided $\mathbf{x} \notin \gamma_i^n$. Both $b(\mathbf{x}, \phi_i^n)$ and the double-layer potential it approximates are discontinuous across γ_i^n and take the value zero on γ_i^n. The integral in equation (34) can also be evaluated exactly.

Noting equation (7) define

$$c(\mathbf{x}, \gamma_2^n) := 2a(\mathbf{x}, \gamma_2^n) + d(\mathbf{x}, \gamma_2^n), \tag{36}$$

where $d(\mathbf{x}, \gamma_2^n)$ denotes an approximation to $\int_{\gamma_2^n} P_{\beta_c}(k(\mathbf{x} - \mathbf{y}))\mathrm{d}s(\mathbf{y})$. Define the approximation d by

$$d(\mathbf{x}, \gamma_2^n) := \begin{cases} h_2^n P_{\beta_c}(k(\mathbf{x} - \mathbf{x}_2^n)), & \mathbf{x} \in \bar{U} \backslash \{\mathbf{x}_2^n\}, \\ h_2^n/2(P_{\beta_c}((0, 0)) + P_{\beta_c}((kh_2^n/2, 0))), & \mathbf{x} = \mathbf{x}_2^n. \end{cases} \tag{37}$$

This approximation is just the midpoint rule when $\mathbf{x} \in \bar{U} \backslash \{\mathbf{x}_2^n\}$. For $\mathbf{x} = \mathbf{x}_2^n$,

$$\int_{\gamma_2^n} P_{\beta_c}(k(\mathbf{x}-\mathbf{y}))\ \mathrm{d}s(y) = \int_{-h_2^n/2}^{h_2^n/2} P_{\beta_c}((\xi, 0))\ \mathrm{d}\xi, \tag{38}$$

$$= 2\int_{0}^{h_2^n/2} P_{\beta_c}((\xi, 0))\ \mathrm{d}\xi, \tag{39}$$

and the approximation $d(x_2^n, \gamma_2^n)$ is the trapezium rule applied to equation (39). This is more accurate than the midpoint rule applied to equation (38) since, while $\hat{P}_{\beta_c}((\xi, 0))$ is a continuous function of ξ, $\partial\hat{P}_{\beta_c}((\xi, 0))/\partial\xi$ has a simple discontinuity at $\xi = 0$ (see reference [17]).

Collocating at the midpoint of each boundary element gives a system of $N_T = 2N_2 + N_1$ linear simultaneous equations for the values p_1^N, p_2^N and q^N at the midpoints of the elements which can be written in matrix form as

$$[\mathbf{A}]\mathbf{p}^N = \mathbf{g}, \tag{40}$$

where $[\mathbf{A}]$ is a $N_T \times N_T$ complex-valued matrix and is given by

$$[\mathbf{A}] = \begin{bmatrix} \frac{1}{2}\mathbf{I} + \mathrm{i}k\mathbf{S}_{11}\mathbf{B} - \mathbf{K}_{11} & \mathbf{K}_{21} - \mathrm{i}k\beta_c\mathbf{S}_{21} & \mathbf{S}_{21} \\ \mathrm{i}k\mathbf{S}_{12}\mathbf{B} - \mathbf{K}_{12} & \frac{1}{2}\mathbf{I} - \mathrm{i}k\beta_c\mathbf{S}_{22} & \mathbf{S}_{22} \\ \mathbf{0} & \mathbf{I} & -\mathbf{S}_{22}^{\beta_c} \end{bmatrix}, \tag{41}$$

$$\mathbf{p}^N = (p_1^N(\mathbf{x}_1^1), \ldots, p_1^N(\mathbf{x}_1^{N_1}), p_2^N(\mathbf{x}_2^1), \ldots, p_2^N(\mathbf{x}_2^{N_2}), q^N(\mathbf{x}_2^1), \ldots, q^N(\mathbf{x}_2^{N_2}))^{\mathrm{T}}, \tag{42}$$

$$\mathbf{B} = \mathrm{diag}(\beta^N(\mathbf{x}_1^1), \ldots, \beta^N(\mathbf{x}_1^{N_1})), \tag{43}$$

$$\mathbf{g} = ((1-\eta(\mathbf{x}_0))g_1(\mathbf{x}_1^1), \ldots, (1-\eta(\mathbf{x}_0))g_1(\mathbf{x}_1^{N_1}), (1-\eta(\mathbf{x}_0))g_2(\mathbf{x}_2^1), \ldots,$$
$$(1-\eta(\mathbf{x}_0))g_2(\mathbf{x}_2^{N_2}), \eta(\mathbf{x}_0)g_{\beta_c}(\mathbf{x}_2^1), \ldots, \eta(\mathbf{x}_0)g_{\beta_c}(\mathbf{x}_2^{N_2}))^{\mathrm{T}}. \tag{44}$$

The elements of the sub-matrices $\mathbf{S}_{ij}$, $\mathbf{K}_{ij}$, $\mathbf{S}_{22}^{\beta_c}$ are given by

$$[\mathbf{S}_{ij}]_{lm} = a(\mathbf{x}_j^l, \gamma_i^n), \qquad l, n = 1, 2, \ldots, N_j, \tag{45}$$

$$[\mathbf{K}_{ij}]_{lm} = b(\mathbf{x}_j^l, \gamma_i^n), \qquad l, n = 1, 2, \ldots, N_j, \tag{46}$$

$$[\mathbf{S}_{22}^{\beta_c}]_{lm} = c(\mathbf{x}_2^l, \gamma_2^n), \qquad l, n = 1, 2, \ldots, N_j, \tag{47}$$

The approximations $a(\mathbf{x}, \gamma_i^n)$, $b(\mathbf{x}, \gamma_i^n)$ $i = 1, 2$ and $c(\mathbf{x}, \gamma_2^n)$ defined above, while relatively simple, are accurate for all positions $\mathbf{x} \in D$ and elements γ_i^n, γ_2^n. In particular one can show, using results on product integration in reference [6], that the error in $a(\mathbf{x}, \gamma_i^n)$, $b(\mathbf{x}, \gamma_i^n)$, and $c(\mathbf{x}, \gamma_2^n)$ is $O(h^{-\epsilon})$ as $h \to 0$ with $\mathbf{x}$ fixed, for all $\epsilon > 0$ and $\mathbf{x} \in U \cup S$ ($\mathbf{x} \in U$ for $c(\mathbf{x}, \gamma_2^n)$). Moreover, for $a(\mathbf{x}, \gamma_i^n)$, $i = 1, 2$, and $c(\mathbf{x}, \gamma_2^n)$ this convergence is uniform in $\mathbf{x}$ and n; this is also true for $b(\mathbf{x}, \gamma_i^n)$, $i = 1, 2$, for > 1.

For very large N_T the cost of solution of the linear equations (40) dominates (requiring $\approx N_T^2/3$ multiplications if Gaussian elimination or a similar method is used). For values of $N_T \approx 1000$ the cost of setting up the matrix [**A**] is important, especially if $\beta_c \neq 0$. When $\beta_c \neq 0$ this cost is dominated by the evaluation of $\hat{P}_{\beta_c}(k(\mathbf{x}_m - \mathbf{x}_n))$ for $m, n = 1, \ldots, N_2$.

Once the values of p^N at the element midpoints have been obtained by solving equation (40), the subsequent calculation of $p^N(\mathbf{x})$ at an arbitrary point in D using equations (32) and (33) has a very much smaller computational cost proportional to N_T.

5. EXPERIMENTAL CONVERGENCE TESTS: ACOUSTIC SCATTERING FROM A RECTANGULAR CUTTING

The numerical solution (32)–(33) of the integral equations IEP1 described in the previous section is tested with a rectangular cutting and fixed frequency $f = 100$ Hz and sound speed $c = 343$ ms^{-1}. γ_j is divided into boundary elements of constant length h_j for $j = 1, 2$.

First, define the errors

$$E_{p_1}^N := p_1 - p_1^N,\ E_{p_2}^N := p_2 - p_2^N,\ E_q^N := q - q^N \quad \text{and} \quad E^N(\mathbf{x}) := p(\mathbf{x}) - p^N(\mathbf{x}). \tag{48}$$

The error on γ_1 and γ_2 will be measured in discrete L_2 norms defined by

$$\| f \|_{\gamma_j} := \left\{ \frac{1}{N} \sum_{m=1}^{N} |f(x_j^m)|^2 \right\}, \qquad j = 1, 2. \tag{49}$$

To illustrate how the numerical scheme converges as $h := \max(h_1, h_2) \to 0$ experimental convergence rates are calculated. These will be assumed to have the asymptotic behaviour

$$\| E_{p_1}^{N_1} \|_{\gamma_1} \sim C_1 h^{\alpha_{P1}},\ \| E_{p_2}^{N_2} \|_{\gamma_2} \sim C_2 h^{\alpha_{P2}},\ \| E_q^{N_2} \|_{\gamma_2} \sim C_3 h^{\alpha_q} \quad \text{and} \quad |E^N(x)| \sim C_4 h^{\alpha}, \tag{50}$$

as $h \to 0$ with h_1/h_2 fixed, where C_j, $j = 1, 2, 3, 4$, α_{p_1}, α_{p_2}, α_q, and α are constants.

To test the method consider the case where the incident wave is the plane wave e^{-ikx_2} rather than the cylindrical wave $G_f(\mathbf{x}, \mathbf{x}_0)$. In this case the term $\eta(\mathbf{x}_0) G_{\beta_c}(\mathbf{x}, \mathbf{x}_0)$ in equation (12) must be replaced by $p_{\beta_c}(\mathbf{x}) = e^{-ikx_2} + (1 - \beta_c)/(1 + \beta_c) e^{ikx_2}$ and the term $(1 - \eta(\mathbf{x}_0)) G_f(\mathbf{x}\ \mathbf{x}_0)$ in equation (13) replaced by 0. The geometry is as in Figure 3, the depth and the width of the cutting being $\lambda = 2\pi/k = 3{\cdot}43$ m. For this geometry the exact solution with the boundary conditions shown in Figure 3 is just $p(\mathbf{x}) = p_{\beta_c}(\mathbf{x})$.

Tables 1–4 show results for the case when β_c has the value $\beta_c = 0{\cdot}37 - 0{\cdot}28$i. Convergence of the numerical scheme is observed with, from Tables 1 and 2, $\alpha_{p_1}, \alpha_{p_2} \approx 1{\cdot}5$ and a convergence rate of $\alpha_q \approx 0{\cdot}5$ observed for q in Table 3. Table 4 shows the convergence rate to be $\alpha \approx 1{\cdot}5$ for the error in $p(\mathbf{x})$ at a typical receiver position $\mathbf{x} = (-0{\cdot}5, 1{\cdot}0)$ m.

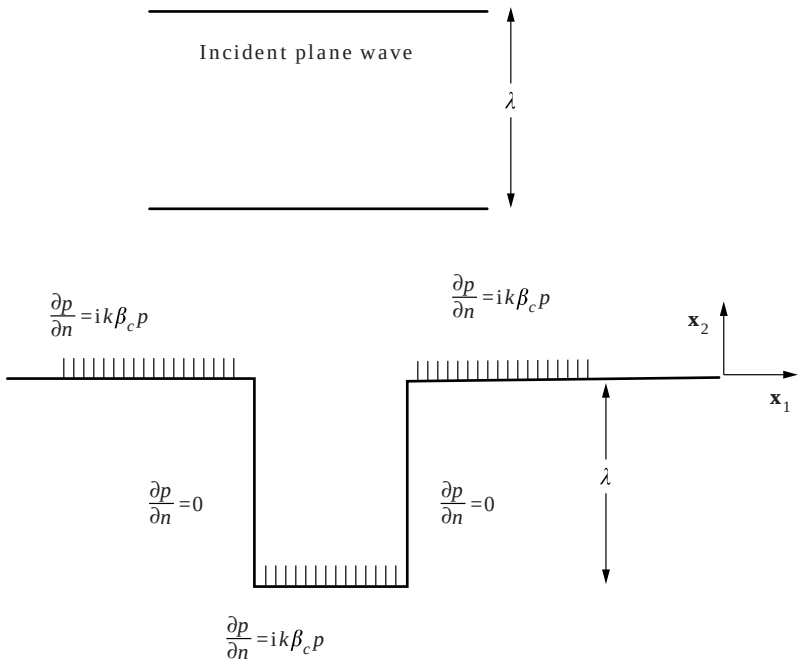

Figure 3. Geometry for plane-wave problem.

Further numerical experiments investigating the rate of convergence of the method for other geometries and incident fields are described in reference [8]: in every case the convergence rate for the error in $p(\mathbf{x})$ at the final receiver position $\mathbf{x}$ is in the range $\alpha = 1{\cdot}5–2{\cdot}0$.

The above convergence has not been analysed theoretically, and there appear to be no convergence or stability results in the literature for collocation methods applied to coupled systems of first and second kind boundary integral equations, of the type IEP1. For convergence results for boundary element collocation methods applied to uncoupled first and second kind integral equations on

TABLE 1

Errors and experimental convergence rate for p_1 for impedance plane-wave problem. Throughout $N_2 = N_1/3$ so that $h_2 = h_1$

N_1	h_1/λ	$\|\|E^N_{p_1}\|\|_{\gamma_1}$	$\|\|E^N_{p_1}\|\|_{\gamma_1} \|\|E^{2N}_{p_1}\|\|_{\gamma_1}$	α_{p_1}
6	1/2	0·53	5·85	2·55
12	1/4	9·0E-2	3·30	1·72
24	1/8	2·7E-2	3·14	1·65
48	1/16	8·7E-3	3·05	1·61
96	1/32	2·8E-3	2·99	1·58
192	1/64	9·5E-4	2·94	1·56
384	1/128	3·2E-4	–	–

TABLE 2

Errors and experimental convergence rate for p_2 for impedance plane-wave problem. Throughout $N_2 = N_1/3$ so that $h_2 = h_1$

N_1	$\|\|E^N_{p_2}\|\|_{\gamma_1}$	$\|\|E^N_{p_2}\|\|_{\gamma_2}/\|\|E^{2N}_{p_2}\|\|_{\gamma_2}$	α_{p_2}
6	0·47	36·46	5·19
12	1·3E-2	2·85	1·51
24	4·5E-3	2·03	1·02
48	2·2E-3	2·48	1·31
96	8·9E-4	2·64	1·40
192	3·4E-4	2·70	1·43
384	1·2E-4	–	–

TABLE 3

Errors and experimental convergence rate for $q = \partial p/\partial n - \mathrm{i}k\beta_c p$ for impedance plane-wave problem. Throughout $N_2 = N_1/3$ so that $h_2 = h_1$

N_1	$\|\|E^N_q\|\|_{\gamma_2}$	$\|\|E^N_q\|\|_{\gamma_2}/\|\|E^{2N}_q\|\|_{\gamma_2}$	α_q
6	3·48	30·1	4·91
12	1·6E-2	2·65	1·4
24	6·0E-3	1·10	0·13
48	5·4E-3	1·29	0·36
96	4·2E-3	1·35	0·43
192	3·1E-3	1·38	0·47
384	2·3E-3	–	–

TABLE 4

Errors and experimental convergence rate for impedance plane-wave problem at receiver position $x = (-0{\cdot}5, 1{\cdot}0)$ m. Througout $N_2 = N_1/3$ so that $h_2 = h_1$

N_1	$\|E^N(x)\|$	$\|E^N\|/\|E^{2N}\|$	α
6	0·34	36·6	5·19
12	9·2E-3	9·23	3·21
24	9·9E-4	2·47	1·35
48	4·0E-4	4·86	2·28
96	8·3E-5	2·86	1·52
192	2·9E-5	3·02	1·6
384	9·5E-6	–	–

polygonal domains, see references [18–21] and the references therein. It is well known that for piecewise constant collocation methods applied to second kind integral equations a convergence rate $\alpha = 2$ is the best that can be achieved (see e.g., reference [6]), which is consistent with the present results.

One would expect some improvements in accuracy and rate of convergence with the numerical method described (though not a higher convergence rate than $\alpha = 2$) if a graded mesh is adopted (see e.g., references [18, 20, 21]), i.e., if smaller boundary elements are used near the corners, at which points the kernels of the integral operators and the solution p have singularities (see reference [22]).

6. RESULTS

Some results are shown in this section illustrating the use of the numerical method described in the previous section to simulate traffic noise propagating out of a cutting onto surrounding flat ground.

For the results shown, the admittance β_c of the absorbing ground is calculated using the Delany and Bazley formulae [23] which give the normalized admittance and complex wavenumber, k_G, of a porous medium as functions of σ/f, where σ is an effective flow resistivity and f is the frequency. The ground is modelled as a porous layer of thickness D on top of a rigid half-space, and it is assumed that the refractive index $|k_G/k| \gg 1$ so that the ground is locally reacting.

The following calculations were carried out in terms of excess attenuation which is defined by

$$EA = -20 \log_{10} \left| \frac{p(\mathbf{x})}{p_{FF}(\mathbf{x})} \right| \text{dB}, \tag{51}$$

where $p(\mathbf{x})$, $p_{FF}(\mathbf{x}) = G_f(\mathbf{x}, \mathbf{x}_0)$ denote actual and free-field acoustic pressure, respectively. Throughout, broad band excess attenuation results are given, which are predictions for a single vehicle, A-weighted, road traffic noise spectrum; see Table 5. These are calculated by combining logarithmic results for each third octave centre frequency between 63 and 3162 Hz. The results are shown as contour plots using UNIRAS software. For the results shown, elements of size $\lambda/5$ (λ the wavelength) were used at each frequency.

It will be recalled that the numerical model assumes a coherent line source of sound while a single vehicle is more realistically modelled as a point source of sound. However, experimental measurements [4, 5] and computer simulations [7] for the related problem of outdoor propagation over noise barriers on a ground plane, suggest that excess attenuation values in the plane through the point source perpendicular to the cutting will be accurately predicted if the point source is replaced by a coherent line source of sound.

6.1. THE EFFECT OF VARYING THE DEPTH OF THE CUTTING

To begin with the effect of varying the depth, H, of the cutting, in the range 0·3 to 1·5 m is determined. (The noise reduction effects of shallow road cuttings are of some current interest in the UK; see reference [24].) Figure 4 shows the geometry used. A source was placed, in all cases, 0·5 m from the floor of the

TABLE 5

Sound pressure level at third octave centre frequencies, at a distance of 1 m *from the source, in free-field conditions*

Frequency (Hz)	Source strength (dB)
63·1	75·3
79·4	80·0
100·0	83·3
125·8	85·7
158·5	88·2
199·5	89·8
251·2	91·0
316·2	91·7
398·1	92·9
501·2	94·5
631·0	95·9
794·3	97·0
1000·0	98·1
1259·0	98·2
1584·9	98·0
1995·3	96·2
2511·9	93·8
3162·3	91·6

cutting, the cutting being 11·0 m wide at the top and 9 m wide at the bottom. The depth, H, of the cutting was varied from 0·3 to 1·5 m. The surface type was the same on the ground surface outside the cutting as on the sides of the cutting. The floor of the cutting was kept rigid. The admittance used for the ground surface and sides of the cutting was that predicted by the Delany and Bazley formulae [23] with an effective flow resistivity of $\sigma = 250\,000$ N s m^{-4} and depth, $D = 0{\cdot}1$ m, values appropriate to grassland.

In each of Figures 5–10 there is an increase in level of around 3 dB(A) relative to that in free-field conditions directly above the cutting, independent of

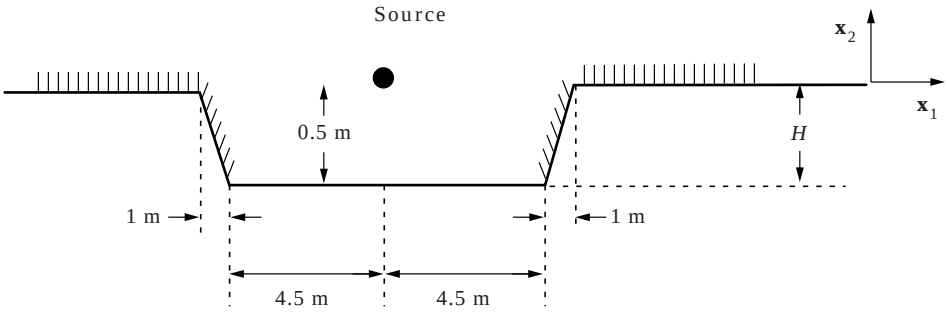

Figure 4. Geometry for cutting height (not to scale).

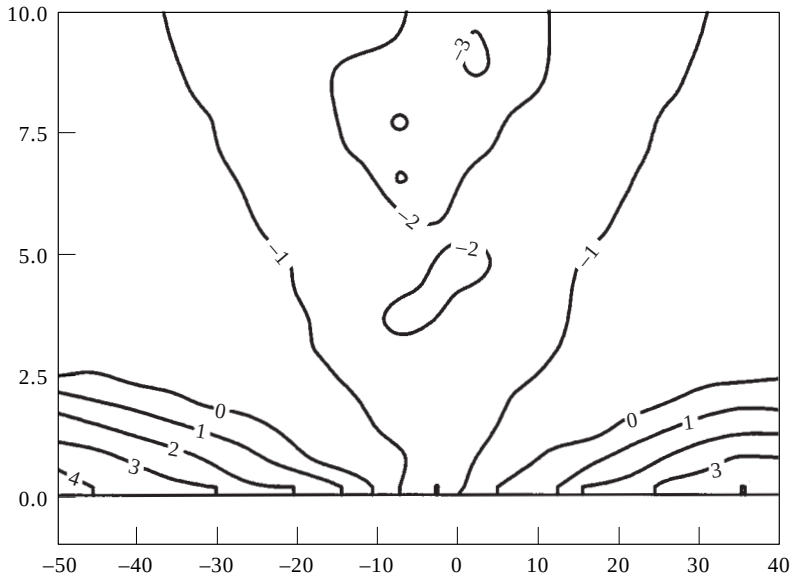

Figure 5. Contours showing excess attenuation for an A-weighted traffic noise spectrum above an impedance plane. The source is at (−5·5, 0·6) m.

the depth of the cutting. In this location the path difference between the direct wave and the wave reflected from the rigid floor of the cutting is so large ($\geqslant 1$ m) that there is a rapid fluctuation between constructive and destructive interference as the frequency increases so that, effectively, the reflection is

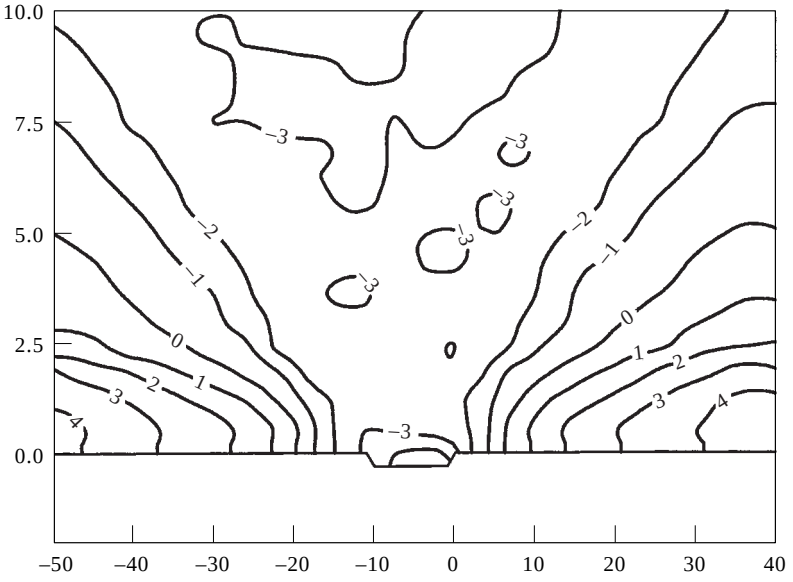

Figure 6. Contours showing excess attenuation for an A-weighted traffic noise spectrum above a cutting of depth 0·3 m. The source is at (−5·5, 0·2) m.

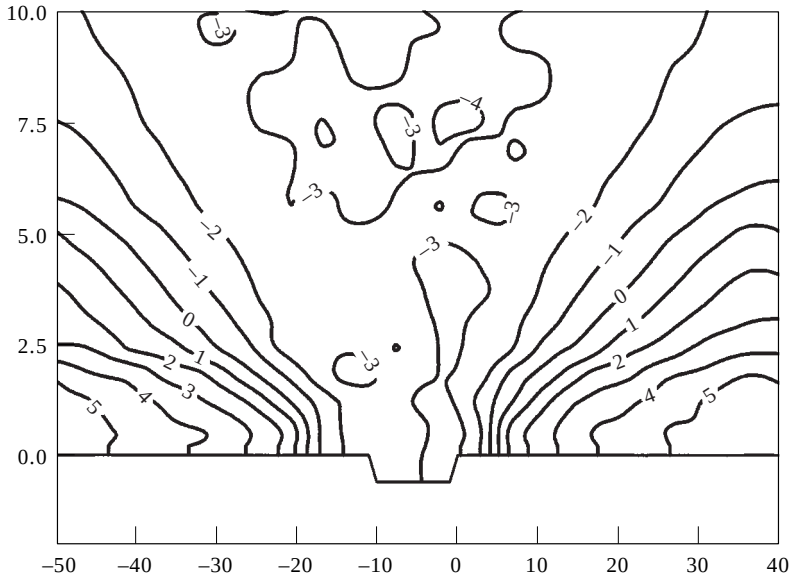

Figure 7. Contours showing excess attenuation for an A-weighted traffic noise spectrum above a cutting of depth 0·6 m. The source is at (−5·5, −0·1) m.

incoherent for a broad band traffic noise spectrum. At ground level about 40 m from the cutting the excess attenuation increases by about 1 dB(A) for every increase in depth of the cutting of 0·3 m.

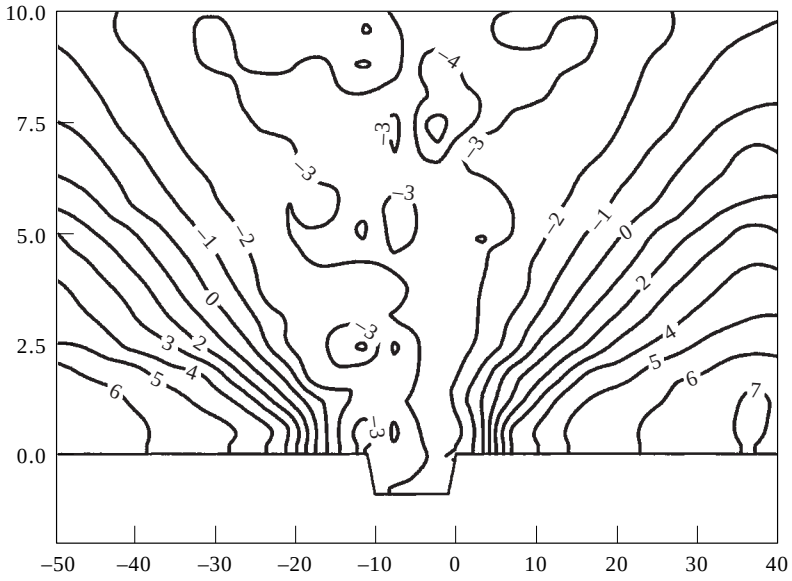

Figure 8. Contours showing excess attenuation for an A-weighted traffic noise spectrum above a cutting of depth 0·93 m. The source is at (−5·5, −0·4) m

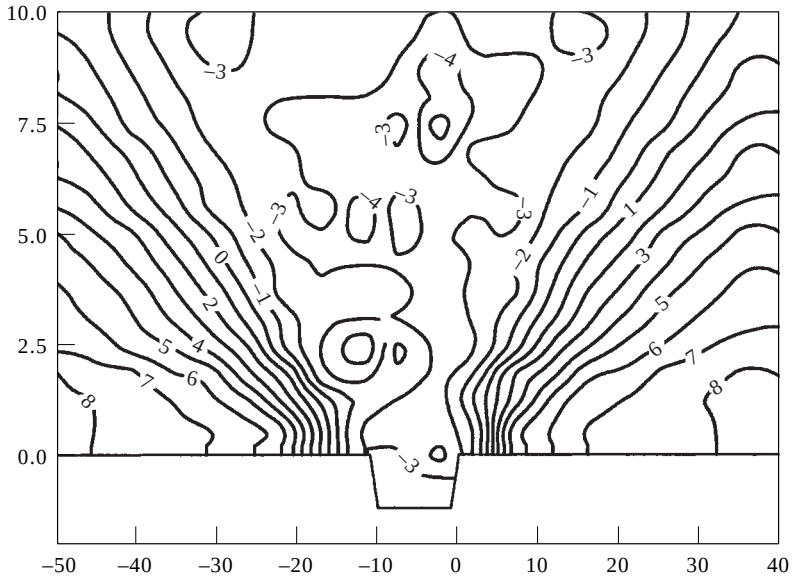

Figure 9. Contours showing excess attenuation for an A-weighted traffic noise spectrum above a cutting of depth 1·2 m. The source is at (−5·5, −0·7) m.

6.2. THE EFFECT OF GROUND ABSORBENCY

Next the effect of ground absorbency is determined Figure 11 shows a second cutting geometry. Again, the floor of the cutting is rigid in the simulations and the sides of the cutting and ground surface have the same surface admittance

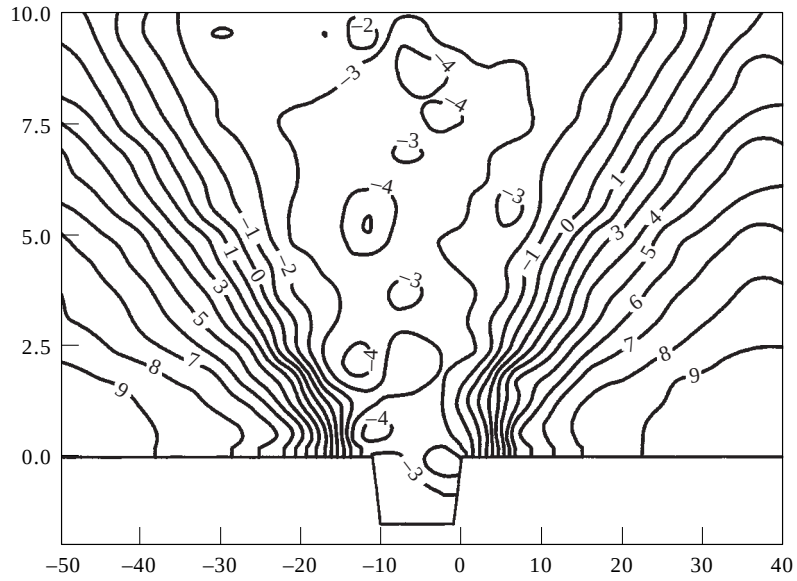

Figure 10. Contours showing excess attenuation for an A-weighted traffic noise spectrum above a cutting of depth 1·5 m. The source is at (−5·5, −1·0) m.

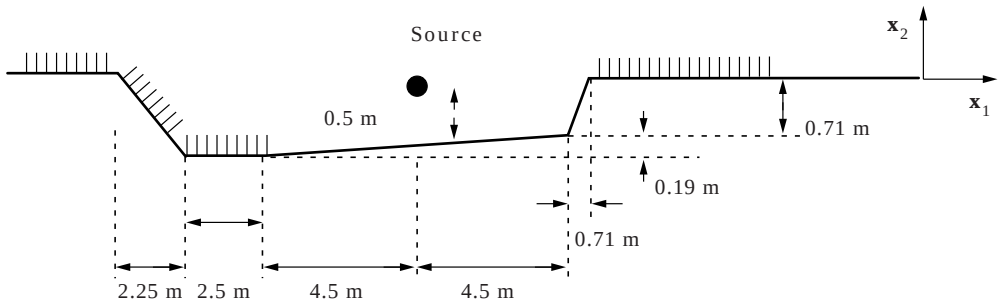

Figure 11. Geometry for a more realistic situation (not to scale).

given by the Delany and Bazley formulae. The cutting is 14·56 m wide and 0·9 m deep. The source is positioned 0·5 m vertically above the road surface.

Figure 12 shows the excess attenuation up to 40 m from the cutting when all surfaces are rigid ($\sigma \to +\infty$ in the Delany and Bazley formulae). Figures 13–15 show the effect of varying the effective flow resistivity in the range $\sigma = 300\,000$–$150\,000$ N sm^{-4}. (Lower values of σ represent more absorbing ground.) For the most absorbent ground and sides of the cutting (Figure 15) an increase in excess attenuation of around 7 dB(A) is observed at 40 m compared to the hard ground case, this reducing to 4 dB(A) for the case $\sigma = 300\,000$ N s m^{-4} (Figure 13). The porous layer depth is kept fixed throughout at $D = 0{\cdot}1$ m.

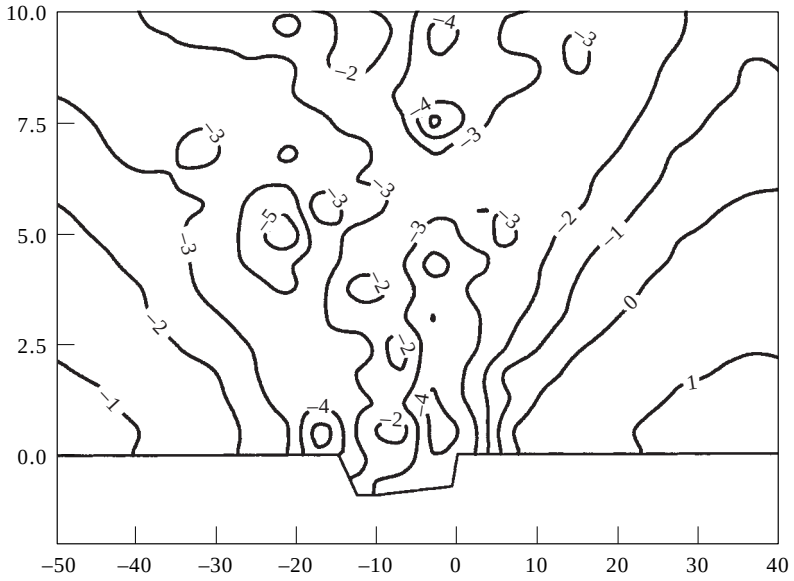

Figure 12. Contours showing excess attenuation for an A-weighted traffic noise spectrum above a rigid cutting.

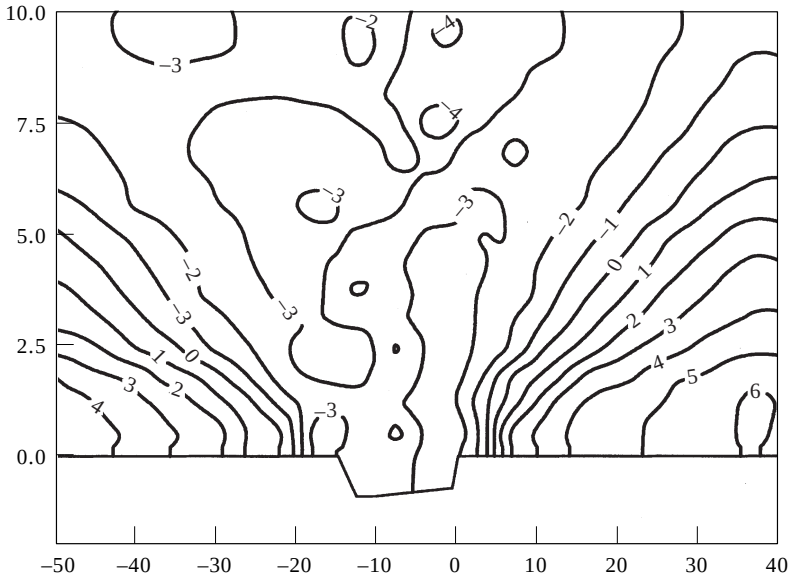

Figure 13. Contours showing excess attenuation for an A-weighted traffic noise spectrum above a cutting with $\sigma = 300\,000\ \mathrm{N\,s\,m^{-4}}$ and depth, $D = 0{\cdot}1$ m.

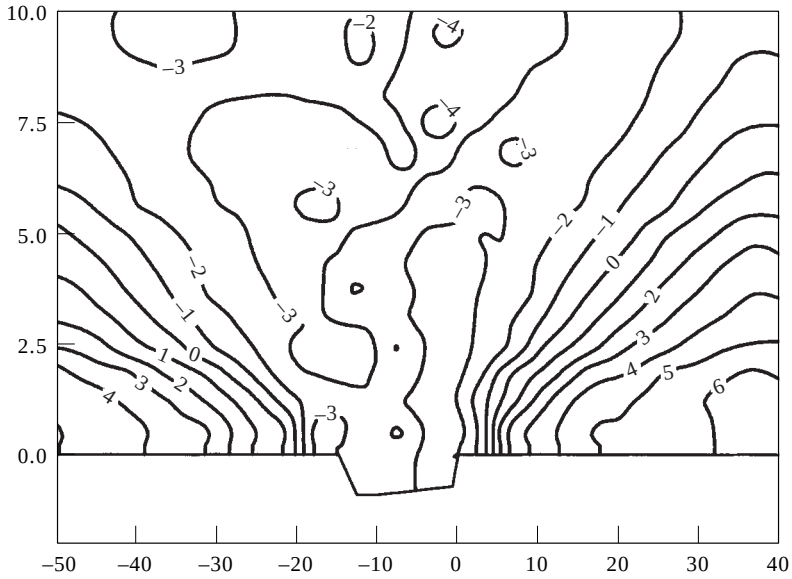

Figure l4. Contours showing excess attenuation for an A-weighted traffic noise spectrum above a cutting with $\sigma = 250\,000\ \mathrm{N\,s\,m^{-4}}$ and depth, $D = 0{\cdot}1$ m.

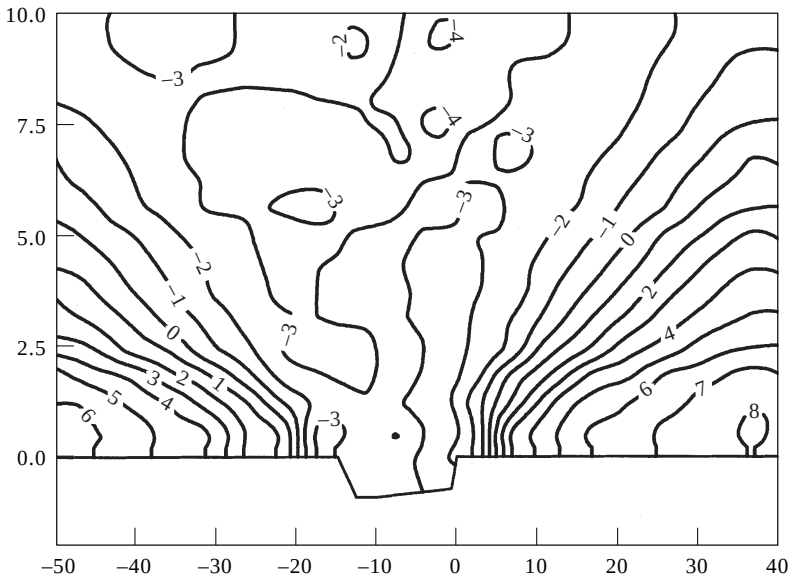

Figure 15. Contours showing excess attenuation for an A-weighted traffic noise spectrum above a cutting with $\sigma = 150\,000\ \mathrm{N\,s\,m^{-4}}$ and depth, $D = 0{\cdot}1$ m.

7. CONCLUSIONS

In this paper the problem of acoustic propagation from a coherent line source within a cutting of arbitrary cross-section and surface impedance out onto a homogeneous impedance plane has been formulated as a boundary value problem for the Helmholtz equation and then reformulated as a coupled system of three boundary integral equations. Equivalence of the boundary value problem and integral equation formulation at all wavenumbers has been demonstrated, so that the formulation does not suffer from irregular frequencies, often encountered in the integral equation formulation of scattering problems.

A boundary element scheme for numerical treatment of the integral equation formulation has been described. Results have been presented demonstrating convergence of the numerical scheme for a simple case where the exact solution can be calculated analytically.

The scope of the numerical scheme to provide predictions of practical interest has been demonstrated by computations for a broad band traffic noise spectrum of propagation from a vehicle source located at 0·5 m above the floor of the cutting out onto surrounding flat ground. The significant effects of varying cutting depth and of varying the absorbency (effective flow resistivity) of the surrounding ground plane have been illustrated.

REFERENCES

1. L.-S. Hwang and E. O. Tuck 1970 *Journal of Fluid Mechanics* **42** , 447–464. On the oscillations of harbours of arbitrary shape.

2. J.-J. LEE 1971 *Journal of Fluid Mechanics* **45**, 372–394. Wave-induced oscillations in harbours of arbitrary geometry.
3. R. P. SHAW 1971 in *Topics in Ocean Engineering* (C. I. Bretschneider, editor) 29–40. Houston, TX: Gulf Publishing Company. Long period forced harbor oscillations.
4. D. C. HOTHERSALL, S. N. CHANDLER-WILDE and N. M. HAJMIRZAE 1991 *Journal of Sound and Vibration* **146**, 303–322. Efficiency of single noise barriers.
5. S. N. CHANDLER-WILDE 1997 *Proceedings of the Institute of Acoustics* **19**, 27–50. Tyndall Medal Lecture: the boundary element method in outdoor noise propagation.
6. G. A. CHANDLER 1979 *Research report, Centre for Mathematical Analysis, Australian National University*. Product integration methods for weakly singular integral equations.
7. D. DUHAMEL 1996 *Journal of Sound and Vibration* **197**, 547–571. Efficient calculation of the 3-dimensional sound pressure field around a noise barrier.
8. A. T. PEPLOW 1995 *Ph.D. thesis*, *University of Bradford*. Integral equation methods for acoustic scattering by infinite obstacles and surfaces.
9. S. N. CHANDLER-WILDE and A. T. PEPLOW 1998 submitted to *Journal of Integral Equations and its Applications*. A boundary integral equation formulation for the Helmholtz equation in a locally perturbed half plane.
10. K. B. RASMUSSEN 1982 *Report Number* 111, *Danish Acoustical Institute*. The effect of terrain profile on sound propagation outdoors.
11. P. J. T. FILIPPI 1983 *Journal of Sound and Vibration* **91**, 65–84. Extended sources radiation and Laplace type integral representation: application to wave propagation above and within layered media.
12. D. HABAULT 1985 *Journal of Sound and Vibration* **100**, 55–67. Sound propagation above an inhomogeneous plane: boundary integral equation methods.
13. S. N. CHANDLER-WILDE and D. C. HOTHERSALL 1995 *Journal of Sound and Vibration* **180**, 705–724. Efficient calculation of the Green function for acoustic propagation over a homogeneous impedance plane.
14. D. COLTON and R. KRESS 1983 *Integral Equation Methods in Scattering Theory*. New York: Wiley-Interscience Publication.
15. D. COLTON and R. KRESS 1998 *Inverse Acoustic and Electromagnetic Scattering* Berlin: Springer; second edition.
16. M. ABRAMOWITZ and I. A. STEGUN 1970 *Handbook of Mathematical Functions*. New York: Dover.
17. S. N. CHANDLER-WILDE and D. C. HOTHERSALL 1991 *Research Report, Department of Civil Engineering, University of Bradford*. On the Green's function for two-dimensional acoustic propagation above a homogeneous impedance plane.
18. M. COSTABEL and E. P. STEPHAN 1987 *Mathematics of Computation* **49**, 461–478. On the convergence of collocation methods for boundary integral equations on polygons.
19. I. G. GRAHAM and Y. YAN 1991 *Journal of the Australian Mathematical Society Series B—Applied Mathematics* **33**, 39–64. Piecewise-constant collocation for first kind boundary integral equations.
20. J. ELSCHNER and I. G. GRAHAM 1995 *Numerische Mathematik* **70**, 1–31. An optimal order collocation method for first kind boundary integral equations on polygons.
21. A. MEIER 1998 *Diplom Thesis, Institut für Angewandte Mathematik, Universität Hannover*. Collocation methods for boundary integral equations for the Helmholtz problem.
22. P. GRISVARD 1985 *Elliptic Problems in Nonsmooth Domains*. Boston, MA: Pitman.
23. M. E. DELANY and E. N. BAZLEY 1970 *Applied Acoustics* **3**, 105–116. Acoustical properties of fibrous absorbent materials.

24. G. R. WATTS 1997 *TRL unpublished report, PR/SE/213/96*. Crowthorne, U.K.: Transport Research Laboratory. Effectiveness of shallow cuttings in controlling road traffic noise.